Journal of Mines, Metals and Fuels, *71(12C): 01-06; 2023. DOI: 10.18311/jmmf/2023/47269*

Print ISSN : 0022-2755

Journal of Mines, Metals and Fuels

Contents available at: *www.informaticsjournals.com/index.php/jmmf*

Detection of Silver Metal Ion by Fluorescence Quenching Studies on Chlorobenzene-Substituted 1,3,4-Oxadiazole Derivatives

R. Chandrashekara[1], T. P. Jyothi[2], Misbhauddin Khan[3], A. Anthony Seleen[4], Lohit Naik[5], Yin Yao[6], Yury Kapelyushin[7], Charles Mbohwa[8] and U. Mahaboob Pasha[8,9]*

[1]Government College for Women, Chintamani - 563125, Karnataka, India
[2]Government First Grade College, K.R. Puram, Bangalore - 560036, Karnataka, India
[3]Government College for Women, Kolar - 563101, Karnataka, India
[4]Government First Grade College, Kolar Gold Fields - 563122, Karnataka, India
[5]Christ University, Bangalore - 560026, Karnataka, India
[6]Electron Microscope Unit, Mark Wainwright Analytical Centre, UNSW Sydney, Sydney, New South Wales - 2052, Australia
[7]South Ural State University (National Research University), Prospekt Lenina, 76, Chelyabinsk, Chelyabinsk Oblast - 454080, Russia
[8]College of Science Engineering and Technology, University of South Africa, Pretoria, South Africa
[9]Presidency University, Bangalore - 560064, Karnataka, India; mahaboobpasha@presidencyuniversity.in

Abstract

Detection of silver nanoparticles by the fluorescence quenching of a chlorobenzene-substituted 1,3,4-oxadiazole derivative, specifically 2-(5-bromonaphtho[2,1-b]furan-2-yl)-5-(2-chlorophenyl)-1,3,4-oxadiazole (2Brx) was investigated by spectroscopic techniques. The fluorescence spectra and fluorescence lifetime of the 2Brx molecule were measured in Dimethyl Sulfoxide (DMSO) by varying concentrations of silver nanoparticles to observe the quenching effect. Key parameters such as Stern-Volmer constants, quenching rate constants, the probability of quenching per encounter and the activation energy of quenching were determined. Time-resolved fluorescence measurements revealed that quenching predominantly occurs through collisional interactions between 2Brx and the silver nanoparticles, with an influence static component. The values of the probability of encounter and the activation energy indicate that the quenching reaction is not exclusively governed by material diffusion. Stern-Volmer plots obtained from steady-state and time-resolved methods demonstrate linear behaviour for the 2Brx and silver nanoparticle systems. The overall results suggest that 2Brx may be effectively used for silver metal ion detections.

Keywords: *1,3,4-Oxadiazole, Activation Energy, Bimolecular Quenching, Diffusion Coefficient*

1.0 Introduction

Fluorescence quenching is a crucial phenomenon in the field of photo-physics and photochemistry. This process provides valuable insights into molecular interactions, distances, and dynamics, making it a vital

*Author for correspondence

tool in various scientific disciplines including materials science, biochemistry and environmental science[1-2]. The 1,3,4-Oxadiazole derivatives are a class of heterocyclic compounds that have garnered significant interest in the field of optoelectronics due to their unique electronic properties, chemical stability and versatile functionality. These compounds exhibit strong fluorescence, high electron affinity and excellent thermal stability, making them ideal candidates for various optoelectronic applications, including Organic Light-Emitting Diodes (OLEDs), organic photovoltaics and organic field-effect transistors. In OLEDs, 1,3,4-oxadiazole derivatives are used as electron transport materials and emitting materials due to their high electron mobility and efficient fluorescence[3-6]. Their ability to facilitate electron injection and transport significantly enhances the performance and efficiency of OLED devices[7-8]. Moreover, the tunable nature of their electronic properties through chemical modification allows for the optimisation of their optical and electrical characteristics, leading to improved device performance. Beyond these applications, 1,3,4-oxadiazole derivatives are also explored for use in sensors, laser dyes and nonlinear optical materials. Their strong fluorescence and tunable electronic properties make them suitable for developing highly sensitive and selective sensors for detecting various chemical and biological analytes. In laser applications, their efficient light-emitting properties are utilised to develop laser dyes with high quantum yields and photostability. Additionally, the nonlinear optical properties of 1,3,4-oxadiazole derivatives open new avenues for their use in advanced photonic devices[9-10].

The rapid advancement of nanotechnologies in recent decades has led to the widespread use of Nanomaterials (NMs) across various industrial applications. This extensive use has raised concerns regarding the environmental impact of Nanoparticles (NPs), as their release and accumulation in the environment are inevitable. NMs pose a potential toxicological risk, with nanosized particles often demonstrating greater toxicity than their larger counterparts[11]. This increased toxicity is due to the unique chemical, physical, and biological properties of NPs, which arise from changes in interaction forces at the nanoscale. The size of NPs is therefore a critical factor influencing their effects on the environment, human health and the biosphere. Among the various NMs, silver nanoparticles (AgNPs) are extensively utilised due to their antimicrobial properties. The broad range of commercial applications for AgNPs has led to a significant increase in their production and subsequent release into the environment. Plants are particularly susceptible to exposure to NPs due to their constant interaction with air, soil and water. Additionally, plants play a crucial role in the food chain, potentially facilitating the bioaccumulation and biomagnification of NPs. Recent research has highlighted the impacts of AgNPs on plant development[12-14].

Given the above, in this study, fluorescence quenching of the highly fluorescent 2Brx molecule was investigated in the presence of silver nanoparticles, to explore its potential applications in optoelectronics.

2.0 Materials and Methods

The chlorobenzene substituted 1,3,4-oxadiazole derivatives like 2-(5-bromonaphtho[2,1-b]furan-2-yl)-5-(2-chlorophenyl)-1,3,4-oxadiazole (2Brx) was synthesised as procedure mentioned in the earlier publication[15]. The molecular structure of the 2Brx is shown in Figure 1. The silver nanoparticle of 30nm size was purchased from Sigma Aldrich. The solvent acetonitrile of HPLC grade was purchased from Sisco Research Laboratories Pvt. Ltd.

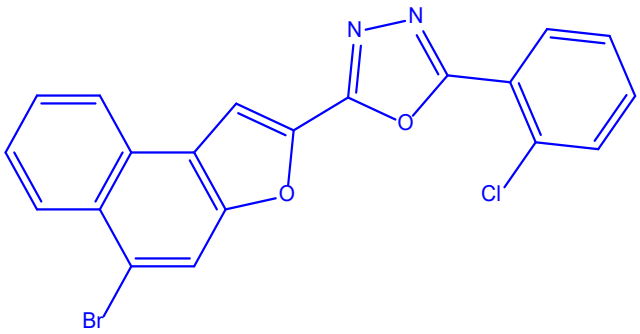


Figure 1. The molecular structure of 2Brx.

3.0 Results and Discussions

The UV-visible absorption spectra of 2Brx were recorded both in the presence and absence of silver nanoparticles (approximately 30nm in size) in DMSO, as shown in Figure 2. From the figure, it is observed that there is no significant change in the absorption spectra of 2Brx. This result indicates that no complex formation occurs

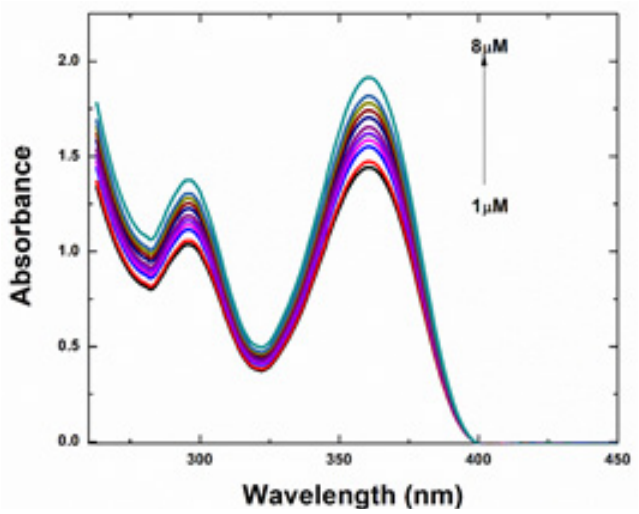


Figure 2. Absorption spectra of 2Brx in the presence and absence of silver nanoparticles.

between 2Brx and the silver nanoparticles. The increase in absorbance of 2Brx is attributed to the surface plasmon resonance of the silver nanoparticles[16].

Figures 3-4 illustrate the fluorescence spectra and fluorescence decay curves of 2Brx in the presence and absence of silver NPs in DMSO, respectively. The fluorescence decay profiles of the fluorophore were fitted to a bi-exponential model, yielding residual c^2 values close to unity. Both the fluorescence intensity and lifetime of the fluorophore decrease with increasing quencher concentration. Therefore, the formation of an excited state complex during the quenching process is ruled out, as no shift is observed in the absorption and emission spectra of any of the molecules in all solvents.

The linearity observed in our Stern-Volmer data, as depicted in Figure 5, indicates that quenching is primarily occurring through a single mechanism, which could be either static or collisional quenching. These mechanisms can be distinguished by conducting time-resolved fluorescence decay measurements across various quencher concentrations. Static quenching is characterized by an unchanged fluorescence decay lifetime, regardless of the quencher concentration. In contrast, collisional quenching creates an additional relaxation pathway for excited molecules, resulting in a decreased average fluorescence lifetime.

Figure 4 clearly shows that the fluorescence decay lifetime diminishes with increasing quencher concentration, providing strong evidence for collisional quenching. The Stern-Volmer constants k_{sv} and are calculated using Equations (1) and (2) from the slopes of the Stern-Volmer plots, as referenced in[16-17]

$$\frac{I_0}{I} = 1 + k_{sv}[Q] \quad (1)$$

and

$$\frac{\tau_0}{\tau} = 1 + k'_{sv}[Q] \quad (2)$$

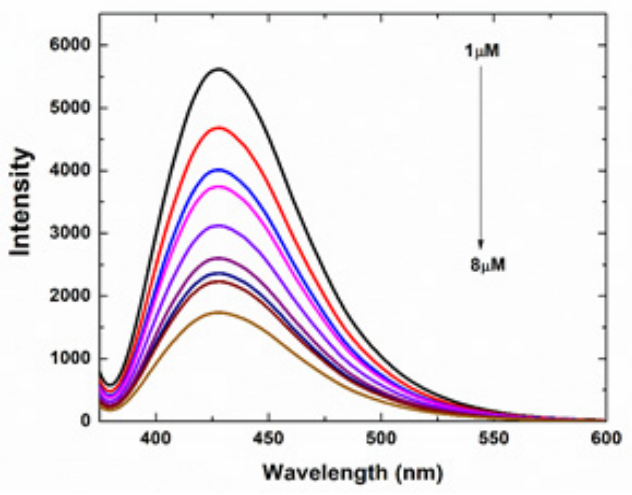


Figure 3. Fluorescence spectra of 2Brx in the presence and absence of silver nanoparticles recorded at an excited wavelength of 366nm.

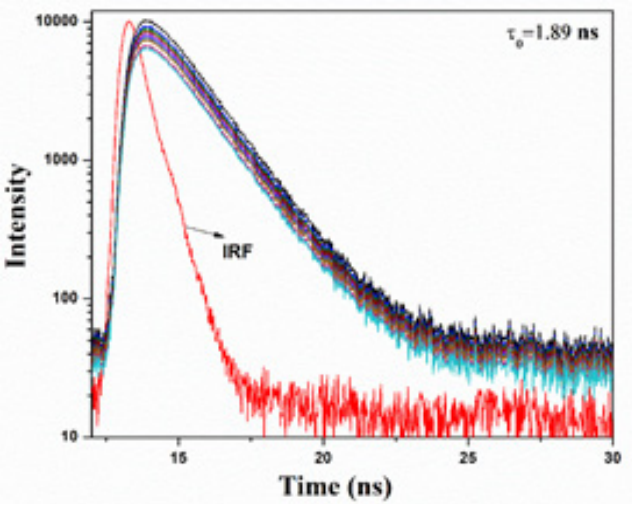


Figure 4. The fluorescence lifetime of 2Brx in the presence and absence of silver nanoparticles recorded at an excited wavelength of 366nm.

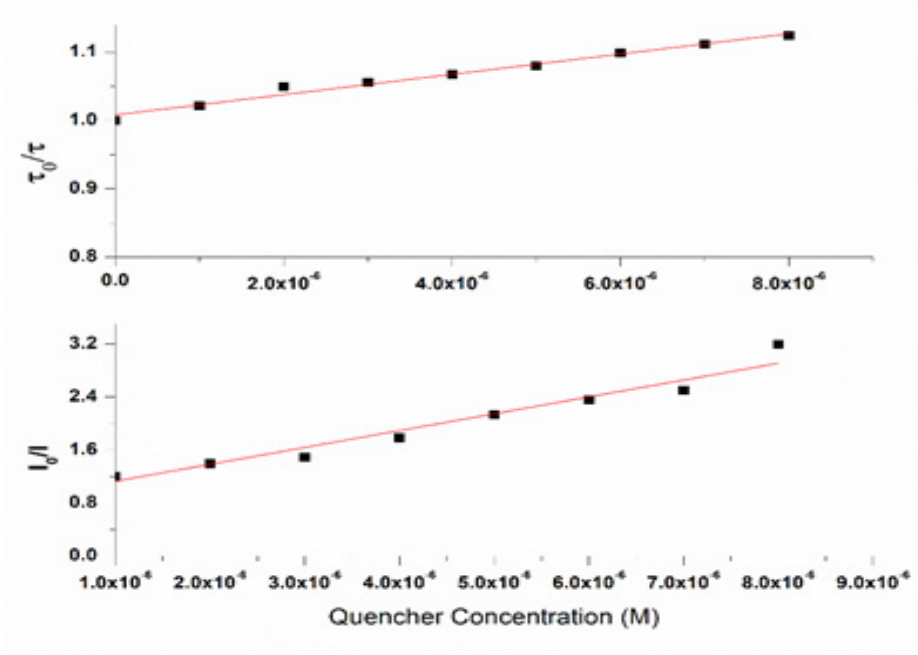


Figure 5. S-V plots of 2Brx.

Table 1. S–V constants, lifetime of the solute in the absence of the quencher and quenching rate parameters, viscosity and diffusion coefficients

k_{sv} (mol^{-1})	$K_q \times 10^{14}$ ($mol^{-1}s^{-1}$)	k'_{sv} (mol^{-1})	$k'_q \times 10^{12}$ ($mol^{-1}s^{-1}$)	$h \times 10^{-3}$ (Pascal)	$D_s \times 10^{-9}$ ($m^{-2}s^{-1}$)	$D_Q \times 10^{-9}$ ($m^{-2}s^{-1}$)	$D \times 10^{-9}$ ($m^{-2}s^{-1}$)
254023	1.344	14870	7.869	0.334	1.052	2.099	3.151

Quenching rate parameters k_q and kq' are calculated according to Equations (3) and (4) respectively.

$$k_{sv} = k_q \tau_0 \quad (3)$$

$$k'_{sv} = k'_q \tau_0 \quad (4)$$

Here, τ_0 and represent the fluorescence lifetimes of the fluorophore in the absence and presence of the quencher, respectively. The Stern-Volmer constants for pure 2Brx and the quenching rate parameters (k_q & k_q') in the presence of silver nanoparticles are provided in Table 1.

The frequency of encounter (k_d)[18] is given as,

$$k_d = 4\pi N' DR\left(1 + \frac{R}{(2D\tau_0)^{\frac{1}{2}}}\right) \quad (5)$$

Where N′ is Avogadro number per mill mole and D is the sum of the diffusion coefficients of solute (D_s) and quencher (D_Q). The diffusion coefficients are obtained from the Stoke-Einstein equation[17] given below.

$$D = \frac{KT}{a\pi\eta R} \quad (6)$$

Here, k represents the Boltzmann constant, T is the absolute temperature and a is the Stokes-Einstein number, which is six for solutes and three for quenchers due to the larger radii of solute molecules compared to solvent molecules. The variable η denotes the solvent viscosity[18]. The parameter R is the sum of molecular radii of 2Brx (R_s) and silver nanoparticles (R_Q) molecules, estimated using the method suggested by Edward[18]. The molecular radius of 2Brx is 4.157 Å, while that of silver nanoparticles is 2.131 Å. The values for the

Table 2. Values of diffusion rate parameter, activation energy for diffusion, activation energy for quenching and probability of quenching per encounter

$k_d \times 10^{10}$ ($mol^{-1}s^{-1}$)	E_d (kcal mol^{-1})	P	E_a (kcal/mol)	P′	E_a (kcal/mol)
1.499	4.214	8965	4.214	52.494	4.214

diffusion coefficient and solvent viscosity are provided in Table 2.

Further, the probability of quenching per encounter (P)[18], was calculated from the steady-state method $(p = \frac{k_q}{k_d})$ and time-resolved method $(p' = \frac{k_d}{k'_d})$ and using this value activation energy was calculated from Equations (7) and (8) and are given in Table 2.

$$E_a = E_d + RT \ln\left(\frac{1}{p} - 1\right) \quad (7)$$

$$E_a = E_d + RT \ln\left(\frac{1}{p'} - 1\right) \quad (8)$$

Here, E_d is the activation energy for diffusion and R is the gas constant.

Figure 5 reveals that the Stern-Volmer constants obtained from the S-V plots differ from each other, indicating the involvement of multiple mechanisms in fluorescence quenching. To verify this, a combined collisional and static quenching model[19] was applied using Equation (9),

$$\frac{I_0}{I} = (1 + k'_{sv}[Q])(1 + k_{sv}[Q]) \quad (9)$$

where all notations retain their usual meanings. The results indicate that fluorescence quenching is primarily due to collisional quenching, with a minor contribution from static quenching.

Figure 5 shows that the Stern-Volmer plots obtained using both steady-state and time-resolved methods are linear and do not exhibit any positive deviation. The bimolecular quenching constants determined from these methods are greater than 10^{10} $mol^{-1}s^{-1}$. This suggests that the fluorescence quenching observed in these dye-quencher systems is attributed to dynamic quenching. Moreover, Table 2 demonstrates that the probability per encounter values (P and P') obtained by both methods are less than one. This further confirms that dynamic quenching is the dominant mechanism between 2Brx and silver nanoparticles. The activation energy for the quenching reaction was calculated using the probability per encounter and the literature values for activation energy related to material diffusion[20]. The results show that the activation energy for the quenching reaction is equivalent to the activation energy for diffusion. This indicates that both activation processes and material diffusion play a significant role in the bimolecular quenching reaction.

4.0 Conclusions

Fluorescence quenching of 2Brx by silver nanoparticles was studied using both steady-state and time-resolved methods in DMSO. The Stern-Volmer plots obtained from these methods demonstrate linear behaviour for the 2Brx and silver nanoparticle systems. The deviation in the Stern-Volmer constants obtained from the two methods suggests that the fluorescence quenching primarily results from collisional quenching, with a minor contribution from static quenching. The probabilities of quenching per encounter, calculated from both methods, are found to be less than unity. This observation indicates that the fluorescence quenching reaction may be influenced by an activation process in addition to material diffusion. Furthermore, the calculated activation energy for diffusion (E_d) is found to be equal to the activation energy for the quenching reaction (E_a) and the frequency of encounter is greater than the bimolecular quenching constant in all solvents. Thus, it can be inferred that the fluorescence quenching reaction is significantly influenced by both the activation energy for quenching and the activation energy for the diffusion process. Overall, the results suggest that the combination of 2Brx and silver nanoparticles holds potential for use in optoelectronic systems.

5.0 References

1. Chakraborty B, Basu S. A systematic progress in probing the excited state using fluorescence spectroscopy. Chem Phys Impact. 2024; 100636. https://doi.org/10.1016/j.chphi.2024.100636
2. Ha T, Tinnefeld P. Photophysics of fluorescent probes for single-molecule biophysics and super-resolution imaging. Annu Rev Phys Chem. 2012; 63(1):595-617. https://doi.org/10.1146/annurev-physchem-032210-103340
3. Paun A, Hadade ND, Paraschivescu CC, Matache M. 1,3,4-Oxadiazoles as luminescent materials for organic light-emitting diodes via cross-coupling reactions. J Mater Chem C. 2016; 4(37):8596-610. https://doi.org/10.1039/C6TC03003C
4. Parra M, Hidalgo P, Carrasco E, Barberá J, Silvino L. New 1,2,4- and 1,3,4-oxadiazole materials: Synthesis and mesomorphic and luminescence properties. Liq Cryst. 2006; 33(8):875-82. https://doi.org/10.1080/02678290600871614
5. Panchamukhi SI, Belavagi N, Rabinal MH, Khazi IA. Synthesis and optoelectronic properties of symmetrical thiophene-based 2,5-disubstituted 1,3,4-oxadiazoles: Highly fluorescent materials for OLED applications. J Fluoresc. 2011; 21:1515-9. https://doi.org/10.1007/s10895-011-0838-y
6. Zhong WY, Song LQ, Zhou B, Zhou HT, Sun HS, Zhang H, Han J. Synthesis, mesomorphic and fluorescent properties of 1,3,4-oxadiazoles/thiadiazoles with a terminal 3-fluoro-4-cyanophenyl group. Tetrahedron. 2023; 144:133579. https://doi.org/10.1016/j.tet.2023.133579
7. Chen Y, Liao CK, Wu TY. Synthesis and characterization of luminescent copolyethers with alternate stilbene derivatives and aromatic 1,3,4-oxadiazoles. Polymer. 2002; 43(17):4545-55. https://doi.org/10.1016/S0032-3861(02)00293-8
8. Li Z, Li W, Keum C, Archer E, Zhao B, Slawin AM, et al. 1,3,4-Oxadiazole-based deep blue thermally activated delayed fluorescence emitters for organic light-emitting diodes. J Phys Chem C. 2019; 123(40):24772-85. https://doi.org/10.1021/acs.jpcc.9b08479
9. Leung MK, Yang WH, Chuang CN, Lee JH, Lin CF, Wei MK, Liu YH. 1,3,4-Oxadiazole containing silanes as novel hosts for blue phosphorescent organic light-emitting diodes. Org Lett. 2012; 14(19):4986-89. https://doi.org/10.1021/ol301734a
10. Linton KE, Fisher AL, Pearson C, Fox MA, Pålsson LO, Bryce MR, Petty MC. Colour tuning of blue electroluminescence using bipolar carbazole-oxadiazole molecules in single-active-layer organic light-emitting devices (OLEDs). J Mater Chem. 2012; 22(23):11816-25. https://doi.org/10.1039/c2jm31825c
11. Tripathi S, Mahra S, Tiwari K, Rana S, Tripathi DK, Sharma S, Sahi S. Recent advances and perspectives of nanomaterials in agricultural management and associated environmental risk: a review. Nanomaterials. 2023; 13(10):1604. https://doi.org/10.3390/nano13101604
12. Wahab A, Muhammad M, Ullah S, Abdi G, Shah GM, Zaman W, Ayaz A. Agriculture and environmental management through nanotechnology: eco-friendly nanomaterial synthesis for soil-plant systems, food safety and sustainability. Sci Total Environ. 2024; 171862. https://doi.org/10.1016/j.scitotenv.2024.171862
13. Ameen F, Alsamhary K, Alabdullatif JA, ALNadhari S. A review on metal-based nanoparticles and their toxicity to beneficial soil bacteria and fungi. Ecotoxicol Environ Saf. 2021; 213:112027. https://doi.org/10.1016/j.ecoenv.2021.112027
14. Rai M, Yadav A, Gade A. Silver nanoparticles as a new generation of antimicrobials. Biotechnol Adv. 2009; 27(1):76-83. https://doi.org/10.1016/j.biotechadv.2008.09.002
15. Ramesh D, Vaidya VP, Kumaraswamy MN, Chandrashekhar C. Synthesis of 2-(8-bromonaphtho[2,1-b]furan-2-yl)-5-aryl-1,3,4-oxadiazoles as potential antimicrobial agents. Int J Pharm Chem Biol Sci. 2014; 4(2).
16. Joseph RL. Principles of fluorescence spectroscopy. 3rd ed. Springer. 2006.
17. Rohatgi-Mukherjee KK. Fundamentals of photochemistry. Wiley Eastern Ltd. 1986.
18. Einstein A. Investigations on the theory of Brownian movement. Dover. 1956.
19. O'Connor DV, Phillips D. Time-correlated single-photon counting. Academic Press. 1984.
20. Kadadevarmath JS, Giraddi TP, Malimath GH, Chikkur GC. Electronic excitation energy quenching of an organic liquid scintillator by carbon tetrachloride in different solvents. J Radiat Meas. 1996; 26:117-26. https://doi.org/10.1016/1350-4487(95)00287-1